Supplementary Information

MicroRNA-211 regulates oxidative phosphorylation and energy metabolism in human vitiligo

Anupama Sahoo[1], Bongyong Lee[1], Katia Boniface[2], Julien Seneschal[2], Sanjaya K. Sahoo[1], Tatsuya Seki[1,3], Chunyan Wang[1], Soumen Das[4] , Xianlin Han[1], Michael Steppie[5], Sudipta Seal[4], Alain Taieb[2] and Ranjan J. Perera[1]*

MATERIALS AND METHODS

Cell lines and tissue culture conditions

Cell lines were primary human epidermal melanocyte-light (HEM-l) (Catalogue # 2200; ScienCell, Carlsbad, CA) cells, the immortalized melanocyte cell line PIG1, and the immortalized line PIG3V derived from the peri-lesional skin of patient with vitiligo. PIG1 and PIG3V cell lines were a kind gift from Dr. Caroline Le Poole, Loyola University, Chicago (IL). HEM-l cells were maintained as described previously (Mazar *et al.*, 2010), and PIG1 and PIG3V cells were grown in Medium 254 (Catalogue #M254500, Life Technologies, Carlsbad, CA) containing HMGS (Catalogue #S0025, Life Technologies) with penicillin and streptomycin.

RNA isolation, cDNA synthesis, and quantitative real-time PCR

Total RNA was isolated from cells using the miRNeasy Mini Kit (Catalogue #217004, Qiagen, Hilden, Germany) with subsequent quantification and integrity analysis using a 2100 Bioanalyzer as described previously (Mazar *et al.*, 2016). Taqman probes were used to quantify hsa-miR-211 using RNU48 primer probes as controls. SYBR green primers were used for the genes listed in Table S5. The Ct values for all genes tested were normalized by the expression of reference gene hypoxanthine phosphoribosyltransferase 1(*HPRT*) unless mentioned otherwise. For patient samples, to isolate total RNA from formalin-fixed paraffin-embedded (FFPE) blocks, eight 20uM sections were collected and RNA was isolated using the miRNA FFPE kit (Catalogue #217504, Qiagen, Hilden, Germany) according to the manufacturer's instructions.

Western blot analysis and melanin content quantification

Equal number of cells were harvested, lysates prepared, and proteins extracted using Radioimmunoprecipitation assay (RIPA) lysis buffer (50 mM Tris pH 7.4; 150 mM NaCl; 1% Triton X-100; 1% sodium deoxycholate;SDS) containing protease inhibitor cocktail and PMSF. The Pierce BCA Protein Assay kit (Thermo Fisher Scientific, Waltham, MA) was used to quantify total protein. Equal amounts of protein were loaded on to 10% SDS polyacrylamide gels and the proteins transferred to nitrocellulose membranes (Whatman International, Maidstone, UK) and incubated with PGC1-α (Catalogue #ST1202, EMD Millipore, Massachusetts, USA), Mitoprofile (Catalogue #ab110413, MitoSciences, Abcam, Cambridge, UK), or Glyceraldehyde-3-Phosphate Dehydrogenase (GAPDH) (Catalogue #sc-25778, Santa Cruz Biotechnology, Inc., Texas, USA) overnight at 4°C followed by incubation

with appropriate secondary antibodies at room temperature for 1 h. Protein bands were detected by chemiluminescence for visualization. GAPDH was used as a loading control. For melanin content, equal numbers of each cell line were pelleted and resuspended in RIPA lysis buffer as above. 30 minutes post lysis, lysates were centrifuged at 13000 g for 15 min, and the resulting pigment pellet was resuspended in NaOH (1 M, in 10% DMSO) solution and incubated at 100 deg C for 30 minutes. The resulting supernatant was used for measurement of melanin at 405 nm in a microplate scanning spectrophotometer (BioTek Instruments, Inc., VT, USA).

Oxygen consumption rate (OCR) and extracellular acidification rate (ECAR)

OCR and ECAR were measured as described previously (Mazar *et al.*, 2016), using the XF Extracellular Flux Analyzer (Seahorse Bioscience, Agilent, Santa Clara, CA) and Seahorse XF Cell Mito Stress Test Kit (Catalogue # 103015-100; Seahorse Bioscience, Agilent, Santa Clara, CA) with minor modifications to the manufacturer's protocols. In brief, 40,000 cells were plated per well in an XF96 cell culture microplate with ten wells used per condition. Final concentrations of reagents were: oligomycin 2 µM, trifluorocarbonylcyanide phenylhydrazone (FCCP) 1 µM, and rotenone-antimycin A 1 µM. The experimental protocol was: loop (3 times), mix (3 min), measure (4 min), loop end, inject port A (for oligomycin); loop (3 times), mix (3 min), measure (4 min), loop end, inject port B (for FCCP); loop (3 times), mix (3 min), measure (4 min), loop end, inject port C (for rotenone-antimycin A); loop (3 times), mix (3 min), measure (4 min), loop end. OCR and ECAR data were analyzed and plotted based upon the averages and standard deviations of all measurements. Each sample was measured in 10 wells per treatment. The assay was performed in triplicate.

Quantification of mitochondrial and genomic DNA content and ROS assay

Equal numbers of each cell line were pelleted and total genomic DNA (nuclear and mitochondrial) was extracted according to the manufacturer's protocol (Quick-gDNA miniprep kit (Catalogue #11-317AC, Zymo Research, Irvine, CA). DNA yields were measured using a NanoDrop spectrophotometer (260/280 nm and 260/230 nm). qRT-PCR was performed using 100 ng of total genomic DNA from all cells using the following primer sets: mtCO1 forward TGGAGCCTCCGTAGACCTAA and reverse TGCGAAGCCTGGTAGGATAA; human 16sRNA forward GCCTTCCCCCGTAAATGATA and reverse TTATGCGATTACCGGGCTCT; human β-globulin forward ACACAACTGTGTTCACTAGC and reverse CAACTTCATCCACGTTCACC. Results are presented relative to nuclear β-globulin labels, which were similar in all cell lines. Intracellular ROS levels were measured in 40,000 cells using the OxiSelect™ Intracellular ROS Assay Kit (Green Fluorescence) (Cell Biolabs Inc., San Diego, CA; Catalogue # STA-342-T).

Luciferase reporter assays

The 3'UTR of human PGC1-α containing one miR211 binding site was cloned into the pcDNA6/Luc/NP vector downstream of the luciferase gene (PGC1-α-3'UTR vector). The PGC1-α UTR was also cloned without the miR211 binding site (PGC1-α-3'UTR-miR211-del). Cloning was performed using the Infusion Cloning kit (Clontech, Mountain View, CA). Primers used were: PGC1-α-3'UTR-F 5'TCCCTAGCTGAGGATGAC3'; PGC1-α-3'UTR-R 5'TAATAAGCGAGTAATGGGTAC3'. PIG3V cells were seeded on a 24-well plate at 50,000 cells/well with 600 ng of either PGC1-α-3'UTR or PGC1-α-3'UTR-miR211-del

vector along with 50 ng pRL-TK (Promega, Madison, WI) expressing Renilla luciferase using Lipofectamine 2000 (Invitrogen). Luciferase activity was measures 48 h post transfection using the Dual–Luciferase reporter assay system (Promega). Firefly luciferase activity was normalized to corresponding Renilla luciferase activity. All transfections were performed in triplicate and normalized with co-transfected Renilla luciferase plasmids.

Cerium oxide nanoparticles

Cerium oxide nanoparticles (CNPs) were prepared using 99.999% pure cerium (III) nitrate hexahydrate as a precursor, maintaining a sterile environment (Das *et al.*, 2012). Briefly, $Ce(NO_3)_3$ $6H_2O$ was dissolved in DNase- and RNase-free distilled water and an excess amount of 30% H_2O_2 was added as an oxidizer. The solution was kept at pH <4 to maintain stability in aqueous solution. CNPs were then thoroughly characterized for the physiological properties including size, surface charge/zeta potential, and surface Ce^{3+}/Ce^{4+} ratio. These well-characterized CNPs were then used for miR-211 loading. The mature miR-211 (sequence 5'-rUrUrCrCrCrUrUrUrGrUrCrArUrCrCrUrUrUrGrCrCrU-3' ,(Mazar *et al.*, 2016) with 3' amine functionalization was purchased from Integrated DNA Technologies (Coralville, IO). Briefly, CNPs were first suspended in DMSO (molecular biology grade), and a 10 times molar excess of 1,1′-carbonyldiimidazole (CDI) was added to the CNPs. The resulting solution was rocked for 1 h to activate the hydroxyl group on the surface of the CNPs. Then, miR-211 was added to the activated CNPs and 10 mM borate buffer (pH 8) added to maintain the pH at ~8 (DMSO <10%) and incubated with rocking for 3 h for conjugation. After conjugation, CNP-miR-211s were dialyzed against DNase- and RNase-free water with three water changes every six hours. The dialyzed CNP-miR-211s were then aliquoted and stored at -20°C until use. CNP-miR-211s were characterized by dynamic light scattering and UV-vis spectroscopy.

RNA sequencing

RNA sequencing was performed at the Genomics Core at the Sanford Burnham Prebys. Briefly, total RNA quality was assessed with the Agilent Bioanalyzer Nano (Agilent Technologies). 1 μg of total RNA was used as starting material to construct RNA-seq libraries using the Illumina TruSeq Stranded Total RNA Library preparation kit as per the instructions. First, total RNA was ribo depleted to remove rRNA from total RNA. The remaining non-rRNA was fragmented using divalent cations at elevated temperature. Following fragmentation, first strand cDNA was synthesized using random primers followed by second-strand synthesis using DNA polymerase I. cDNA was ligated with index adapters for each sample followed by purification and enrichment by PCR to create the final library. The quality and quantity of the libraries were analyzed using the Agilent Bioanalyzer and Kapa Biosystems qPCR. Multiplexed libraries were pooled, and single-end 50 bp sequencing was performed on one flow-cell of an Illumina HiSeq 2500.

Lipid extraction and analysis

Cell samples were re-suspended in 300 μL PBS and homogenized for 1 min using a disposable soft tissue homogenizer. Protein assays on individual homogenates were performed using a bicinchoninic acid (BCA) protein assay kit (Pierce, Rockford, IL). Lipid extraction from the remaining homogenate was performed using a modified Bligh and Dyer extraction procedure as described previously (Cheng *et al.*, 2006). A mixture of lipid internal standards was added prior to lipid extraction based on the total protein content of each sample.

Lipid extract was re-suspended into 400 μL chloroform/methanol (1:1, v/v) per mg of protein and flushed with nitrogen, capped, and stored at -20°C for mass spectrometry. A triple-quadrupole mass spectrometer (Thermo TSQ VANTAGE, San Jose, CA) equipped with a Nanomate device (TriVersaNanoMate, Advion Bioscience Ltd., Ithaca, NY) and Xcalibur system software was used as previously described [ref]. Lipid extracts were further diluted to a final concentration of ~500 fmol/μL and then infused into the electrospray ionization source through an automated nanospray device. Typically, signals were averaged around 3 min periods in the profile mode for each full-scan MS spectrum, and 3 to 5 min periods of signal averaging in the profile mode were employed for each tandem mass spectrum. For tandem MS, the collision energy varied with the classes of lipids as described previously (Han and Gross, 2005), and the collision gas pressure was set at 1.0 mTorr. All the acquired MS data processing was conducted using a custom-programmed Microsoft Excel macro as previously described (Yang *et al.,* 2009), with due consideration of lipidomics principles (Wang *et al.,* 2016, Yang and Han, 2011).

Metabolomics analysis

Metabolomics analysis was performed at the metabolomics core facility at SBP, Lake Nona. In brief, cell cultures containing equal numbers of cells were rinsed with PBS and liquid nitrogen μ (LN_2) was directly added to quench metabolism and efficiently lyse all cellular compartments. After boiling off the LN_2, the frozen material (slush) was quantitatively transferred using a cell lifter and razor blade into a 50 mL conical tube submerged in dry ice and delivered to the Metabolomics Core. Samples were thawed on ice, vortexed, and protein concentrations determined. For amino acids, acylcarnitine, and organic acid analyses, cell lysates were treated with acetonitrile/0.6% formic acid. Amino acids and acylcarnitines were extracted in methanol, and organic acids were extracted in ethyl acetate. All metabolites were derivatized prior to LC/MS/MS analysis. Authentic heavy isotope-labeled internal standards were used for quantitation purposes. Acetyl- and malonyl-CoA were extracted from cell lysate in 5% trichloroacetic acid. Samples were cleaned using solid-phase extraction prior to LC/MS/MS analysis.

Data analysis

The raw reads (FASTQ files) were aligned to the reference genome using TopHat version v2.0.13 (Trapnell *et al.,* 2009) with RefSeq annotations and the "—no-novel-juncs" option. Ambiguous reads mapping to more than one genomic region and reads with MAPQ scores less than 10 were removed. The UCSC human genome version 38 (hg38) and the corresponding RefSeq annotations were used as reference and for mRNA transcript quantification. The annotation and coordinates of the lncRNAs from GenCode (Release 24, GRCh38) were applied for lncRNA transcript quantification. Transcript quantification was performed in Partek Genomics Suite (version 6.6, Partek Inc., St. Louis, MI) and the raw read counts and normalized read counts (RPKM: reads per kilobase per million mapped reads (Mortazavi *et al.,* 2008)) were obtained. The raw count information for all mRNA and lncRNA transcripts was filtered, with transcripts not presenting read counts in all samples filtered from further analysis. The remaining transcripts were analyzed with the BioConductor DESeq package (Anders and Huber, 2010) to detect differential expression between the conditions. Transcripts detected in at least one sample (RPKM>1), fold change over 2, and with p-values <0.05 were considered as significant differential expression.

Supplementary Figures

Supplementary Tables

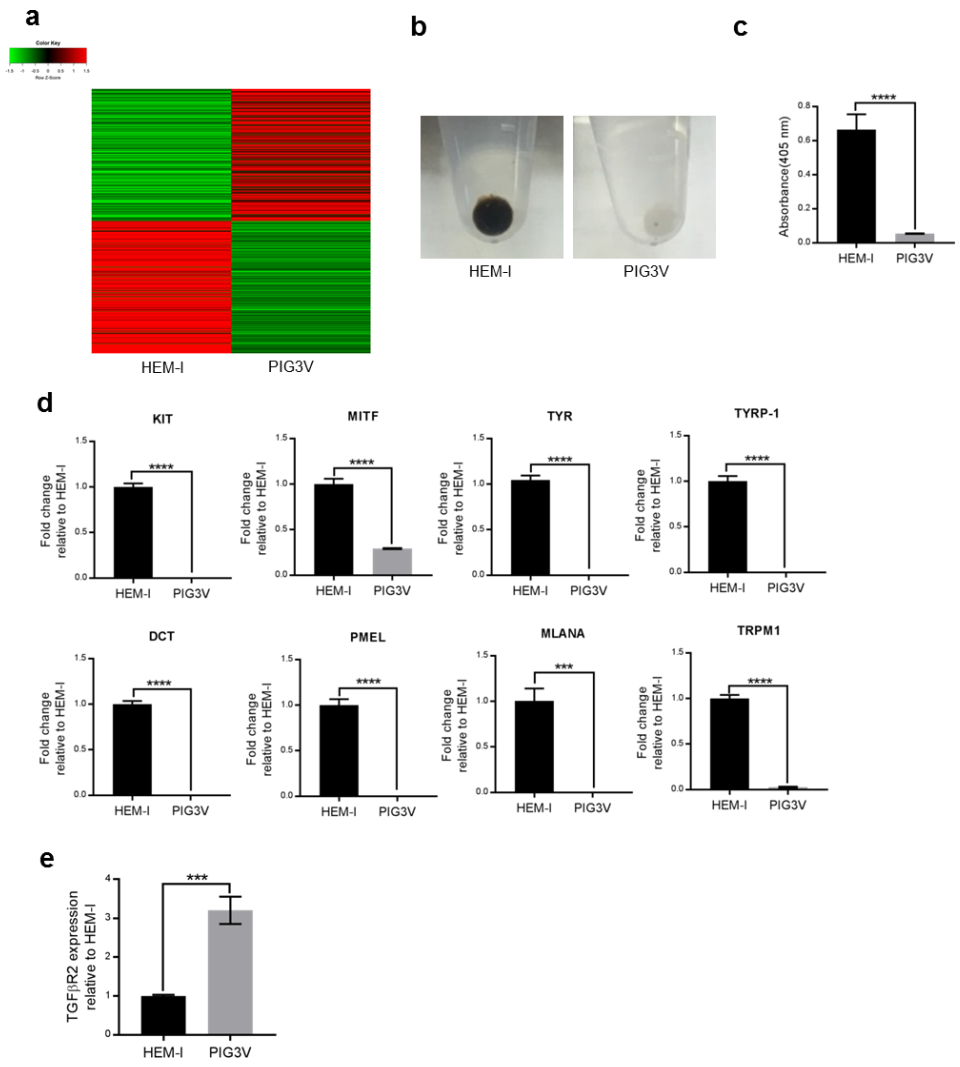

Figure S1. Characterization of vitiligo melanocytes versus normal melanocytes (**a**) Hierarchical clustering of primary melanocytes (HEM-l) and vitiligo (PIG3V) cells. (**b**) Cell pellets of HEM-l and PIG3V cells. (**c**) HEM-l and PIG3V cells were analyzed for melanin content. Graph depicts absorbance of dissolved pigments of each cell type at 405nm. (**d**) HEM-l and PIG3V cells were analyzed for expression of the indicated genes by quantitative RT-PCR. (**e**) HEM-I and PIG3V cells were analyzed for expression of *TGFβR2* by quantitative RT-PCR. Graphs in d and e show fold change in the indicated gene's expression compared to its expression in HEM-l cells. The Ct values were normalized by the expression of a reference gene *HPRT*. Results shown are mean ± SDM and are representative of at least three independent experiments. Student's t-test was performed to detect between-group differences. P values: ****<0.0001

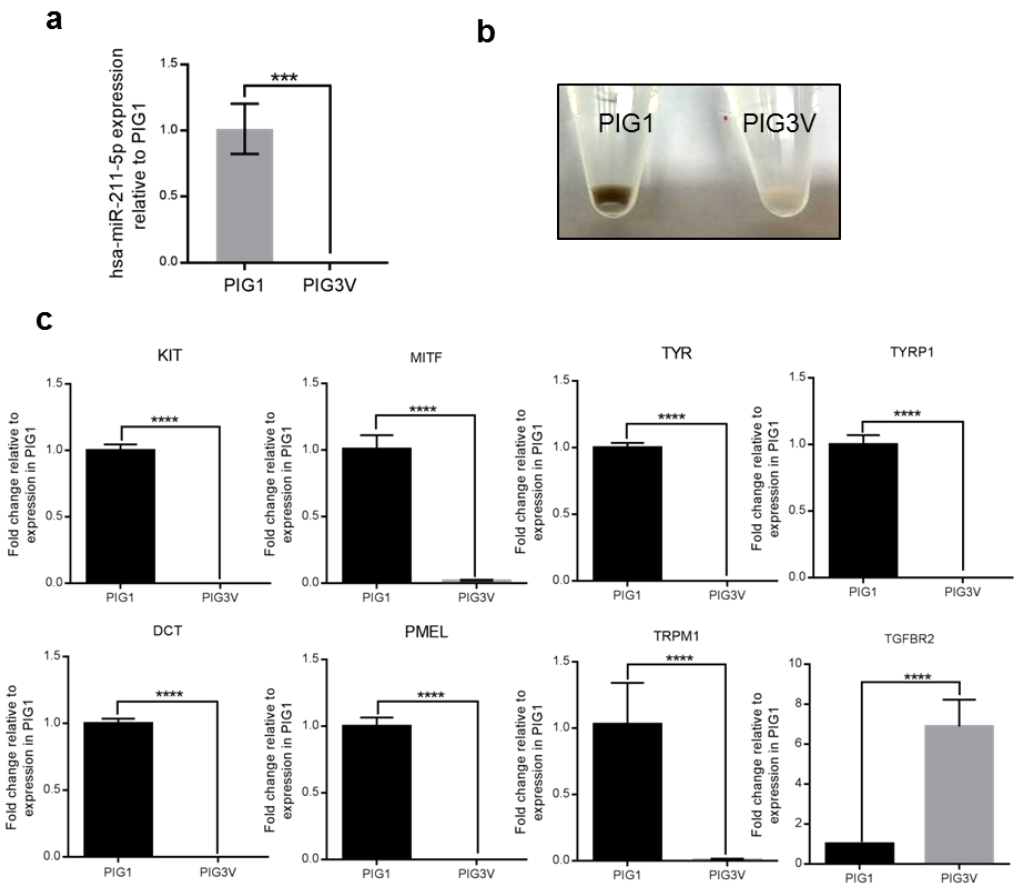

Figure S2. miR-211 and pigmentation genes in PIG1 and PIG3V cells. (**a**) PIG1 and PIG3V cells were analyzed for expression of hsa-miR-211 by quantitative RT-PCR. Graph shows fold change in miR-211 expression compared to its expression in PIG1 cells. (**b**) Cell pellets of PIG1 and PIG3V cells. (**c**) PIG1 and PIG3V cells were analyzed for expression of the indicated genes by quantitative RT-PCR. Graphs show fold change in the indicated gene's expression compared to its expression in PIG1 cells. The Ct values in (**a**) and (**c**) were normalized by the expression of a reference small non-coding RNA, *RNU48* and a reference gene *HPRT*, respectively. Results shown are mean ± SDM and are representative of at least three independent experiments. Student's t-test was performed to detect between-group differences. P values: ***<0.001; ****<0.0001.

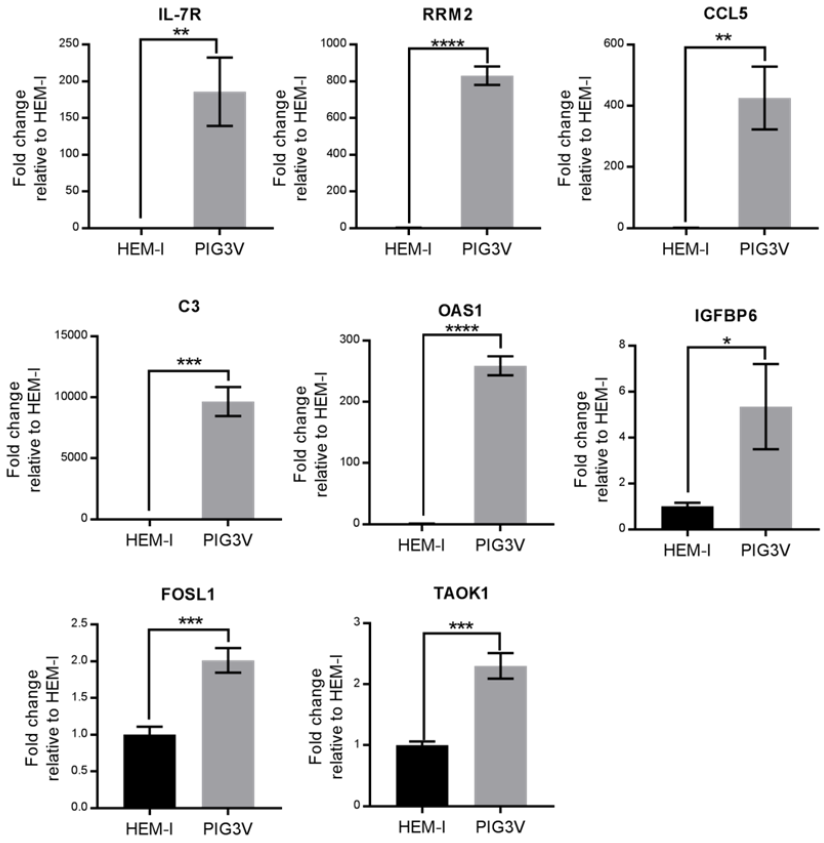

Figure S3. Confirmation of human vitiligo patient gene expression data (see main Table 2) by qPCR in HEM-l and PIG3V cells. HEM-I and PIG3V cells were analyzed for expression of the indicated genes by quantitative RT-PCR. Graphs show fold change in the indicated gene's expression compared to its expression in HEM-I cells. The Ct values were normalized by the expression of a reference gene *HPRT*. Results shown are mean ± SDM and are representative of at least three independent experiments. Student's t-test was performed to detect between-group differences. P values: *<0.05; **<0.01; ***<0.001; ****<0.0001

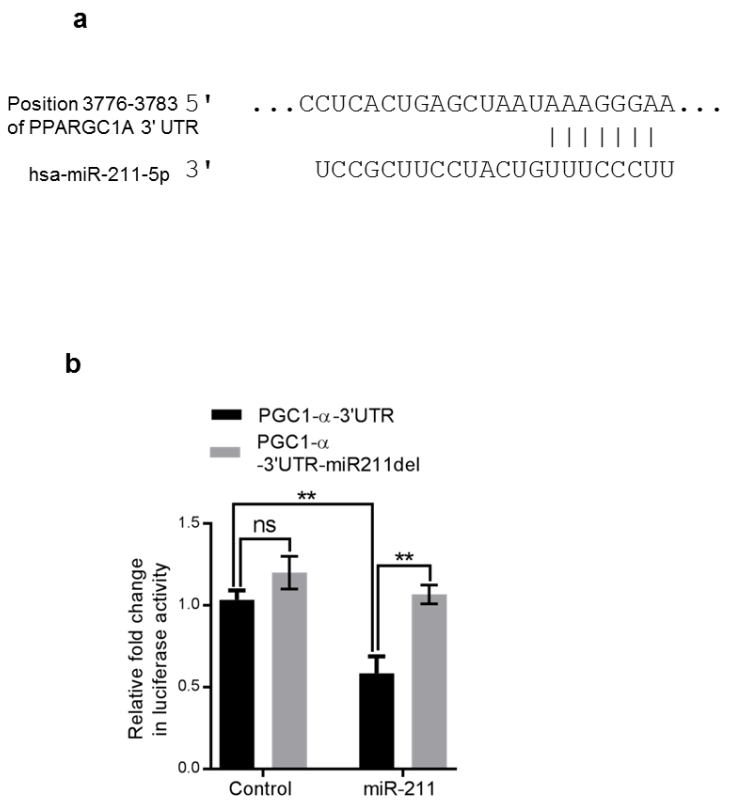

Figure S4. miR-211 targets PGC1-α 3'UTR locus. (**a**) Predicted miR-211 binding site at the PGC1-α 3'UTR locus in TargetScan (human PPARGC1A ENST00000264867.2 3' UTR length: 3801bp) (**b**) HEK293 cells were transfected with luciferase expression vectors (pcDNA6-Luc) containing either the PGC1-α-3'UTR or PGC1-α-3'UTR-miR211-del (miR-211 binding site deleted) with vector only or miR-211 expression vector. 48 h post transfection, cells were analyzed for luciferase activity. Graph shows relative fold change in luciferase activity compared to HEK293 cells transfected with PGC1-α-3'UTR containing luciferase expression plasmid. All transfections were performed in triplicates and normalized with co-transfected Renilla luciferase plasmids. Results shown in (**b**) are mean ± SDM and representative of at least three independent experiments. Student's t-test was performed to detect between-group differences. P values: **<0.01

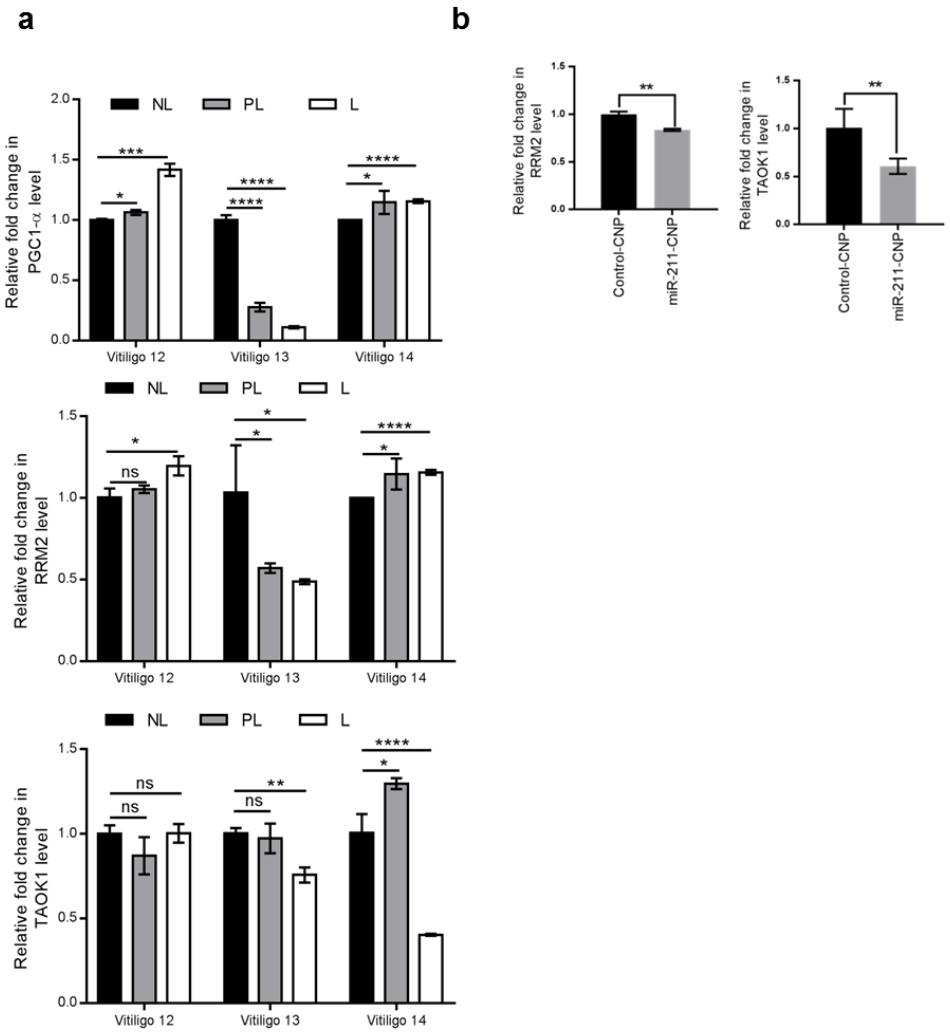

Figure S5. Analysis of putative miR-211 target genes in non-lesional, peri-lesional, and lesional areas of patients with vitiligo. (**a**) Total RNA from non-lesional (NL), peri-lesional (PL), and lesional (L) regions from three patients with vitiligo was analyzed for the expression of indicated genes (*PPARGC1A*, *RRM2*, and *TAOK1*) by quantitative RT-PCR. Graph shows fold change in indicated gene expression in each patient compared to it's expression in the corresponding NL region. The Ct values were normalized to the average expression of four reference genes (*GAPDH*, *ACTB*, *HPRT*, and *TBP*). Results shown are mean ± SDM. (**b**) PIG3V cells were treated with either miR-211-CNP or control CNP. 24 h post treatment, cells were analyzed for indicated gene expression. The Ct values were normalized by the expression of reference gene *HPRT*. Data are depicted as fold changes in gene expression compared to their expression in untreated PIG3V cells alone. Results shown in (**b**) are mean ± SDM and representative of at least three independent experiments. Student's t-test was performed to detect significant differences as indicated. P values::*<0.05; **<0.01; ***<0.001; ****<0.0001

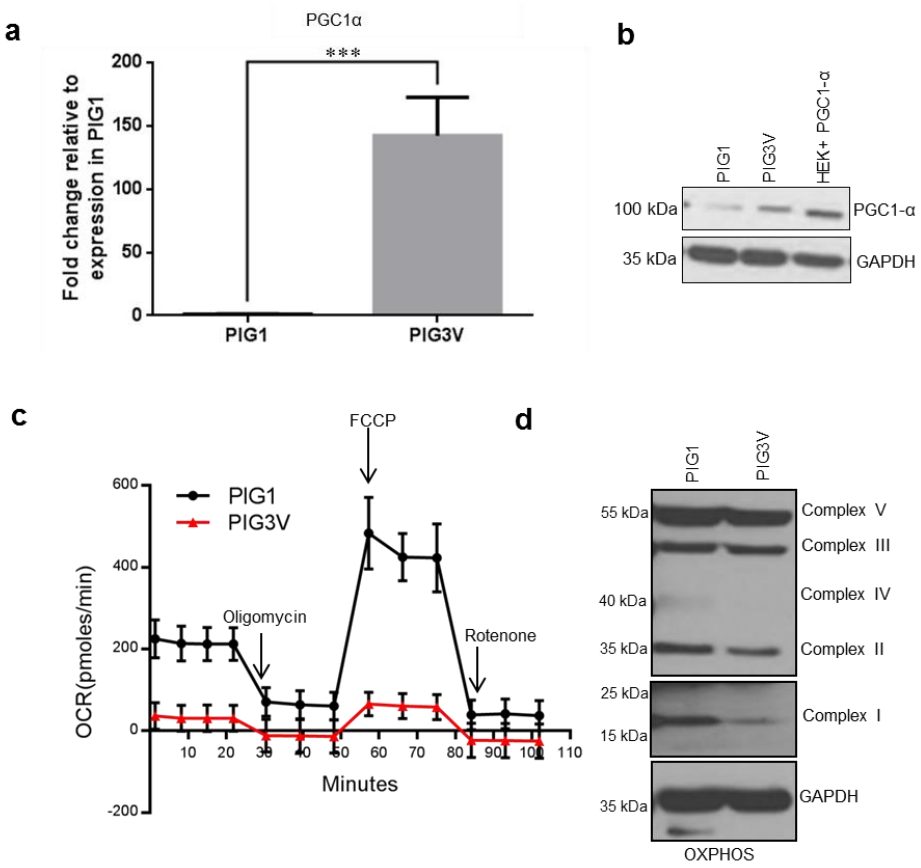

Figure S6. Increased PGC1-α expression and reduced oxidative capacity in PIG3V cells compared to PIG1 cells. (**a-b**) PIG1 and PIG3V cells were analyzed for PGC1-α expression by quantitative RT-PCR (**a**) and western blot analysis (**b**). The Ct values in (a) were normalized by the expression of a reference gene *HPRT* and are depicted as a fold change in PGC1-α expression compared to its expression in PIG1 cells. Student's t-test was performed to detect significant differences as indicated. P values ***<0.001 (**c**) Oxygen consumption rate (OCR) and extracellular acidification rate (ECAR) were analyzed using the Seahorse XF analyzer in PIG1 and PIG3V cells. OCR and ECAR were measured in untreated cells followed by treatment with oligomycin (2uM) and follow-up treatment with FCCP (1uM) and finally rotenone/antimycin A (1uM) cocktail. Each sample was measured in 10 wells per treatment. The assay was performed in triplicate. (**d**) PIG1 and PIG3V cell lysates were analyzed for the expression of the indicated mitochondrial complex subunits by western blot analysis. GAPDH was used as a loading control. Results shown are representative of at least three independent experiments

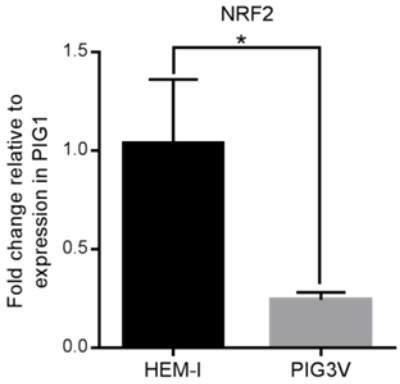

Figure S7. Defective *NRF2* expression in PIG3V cells. HEM-l and PIG3V cells were analyzed for expression of *NRF2* by quantitative RT-PCR. Graphs show fold changes in expression compared to HEM-l cells. Results shown are mean ± SDM and representative of at least three independent experiments. Student's t-test was performed to detect significant differences. P value: *<0.05

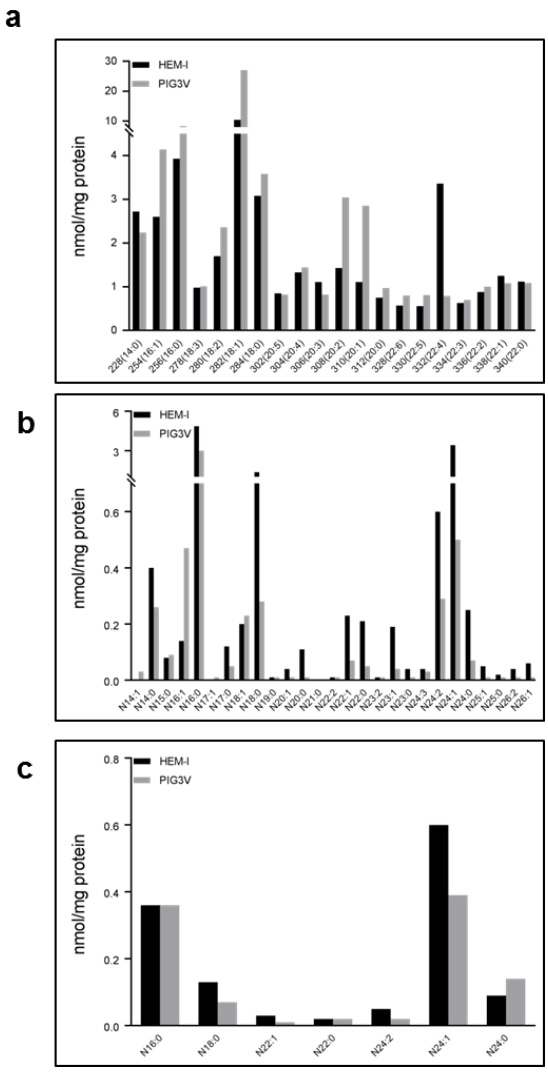

Figure S8. Lipidomics analysis of HEM-I and PIG3V cells. (**a-c**) Graphs depict changes in fatty acid chains for different lipid families

Table S1a. Top twenty upregulated genes in PIG3V compared to HEM-l cells.

Gene	Gene Description	Log2FC (PIG3V/HEM-l)	p-value
AKR1C3	aldo-keto reductase family 1, member C3	11.1	<0.0001
TOP2A	topoisomerase (DNA) II alpha	10.7	<0.0001
THBS1	thrombospondin 1	9.3	<0.0001
FN1	fibronectin 1	8.0	0.0001
CENPF	centromere protein F	8.0	<0.0001
FBN2	fibrillin 2	6.6	<0.0001
ATAD2	ATPase family, AAA domain containing 2	6.2	<0.0001
HSP90B1	heat shock protein 90kDa beta family member 1	4.6	<0.0001
TPR	translocated promoter region, nuclear basket protein	4.6	<0.0001
LAMB1	laminin subunit beta 1	4.2	<0.0001
DEK	DEK proto-oncogene	3.7	<0.0001
PRKDC	protein kinase, DNA-activated, catalytic polypeptide	3.7	0.0001
HSP90AA1	heat shock protein 90kDa alpha family class A member 1	3.4	0.0004
UTRN	utrophin	3.0	<0.0001
MYH9	myosin, heavy chain 9, non-muscle	2.6	0.0075
PPARGC1A	PPARG coactivator 1 alpha	2.4	0.0004
FADS1	fatty acid desaturase 1	2.4	0.0036
CANX	calnexin	2.2	0.0093
MCM3	minichromosome maintenance complex component 3	2.0	0.0003
MCAM	melanoma cell adhesion molecule	1.9	0.0015

Table S1b. Top twenty downregulated genes in PIG3V compared to HEM-l cells.

Gene	Gene Description	Log2FC (PIG3V/HEM-l)	p-value
TYR	tyrosinase	-18.7	<0.0001
PMEL	premelanosome protein	-13.2	<0.0001
DCT	dopachrome tautomerase	-11.1	<0.0001
TYRP1	tyrosinase related protein 1	-10.4	<0.0001
TRPM1	transient receptor potential cation channel subfamily M member 1	-9.6	<0.0001
PSAP	prosaposin	-5.1	<0.0001
IGFBP7	insulin like growth factor binding protein 7	-3.4	0.0005
SCARNA10	small Cajal body-specific RNA 10	-3.4	<0.0001
ATP1A1	ATPase Na+/K+ transporting subunit alpha 1	-3.1	0.0001
FTL	ferritin, light polypeptide	-2.9	0.0037
SAT1	spermidine/spermine N1-acetyltransferase 1	-2.9	<0.0001
CD63	CD63 molecule	-2.8	0.0004
LMNA	lamin A/C	-2.6	0.0001
PSAP	prosaposin	-2.6	0.0080
FSTL1	follistatin like 1	-2.5	0.0021
LGALS1	galectin 1	-2.3	0.0026
BSG	basigin (Ok blood group)	-2.3	0.0021
FAT1	FAT atypical cadherin 1	-2.0	<0.0001
QPRT	quinolinate phosphoribosyl transferase	-2.0	0.0001
DDB1	damage specific DNA binding protein 1	-2.0	0.0054

Table S2. List of major pigmentation pathway genes downregulated in PIG3V cells compared to normal melanocytes

Gene	Gene description	Log2FC (PIG3V/HEM-l)	p-value
TYR	Tyrosinase	-18.7	<0.0001
PMEL	premelanosome protein	-13.2	<0.0001
DCT	Dopachrome tautomerase	-11.1	<0.0001
MLANA	Melan-A	-10.9	<0.0001
c-KIT	KIT proto-oncogene receptor tyrosine kinase	-10.5	<0.0001
TYRP1	Tyrosinase related protein 1	-10.4	<0.0001
MITF	Microphthalmia -associated transcription factor	-6.1	<0.0001
PAX3	Paired box 3	-3.7	<0.0001

Table S3. Differential expression of genes involved in cell cycle progression in PIG3V and HEM-l cells

Gene	Gene Description	Log2FC (PIG3V/HEM-l)	p-value
CHEK1	cell cycle checkpoint kinase	6.8	<0.0001
KNTC1	kinetochore associated 1	3.6	<0.0001
MCM4	minichromosome maintenance complex component 4	3.2	<0.0001
CDK6	cyclin-dependent kinase 6	3.1	<0.0001
CUL3	cullin 3	2.9	<0.0001
RBBP8	retinoblastoma binding protein 8	2.8	<0.0001
CDKN2B	cyclin-dependent kinase inhibitor 2B	2.7	<0.0001
HPRT1	hypoxanthine phosphoribosyl transferase 1	2.6	<0.0001
MCM3	minichromosome maintenance complex component 3	2.3	0.0001
CKS1B	CDC28 protein kinase regulatory subunit 1B	2.1	0.0206
MCM2	minichromosome maintenance complex component 2	2.0	0.0001
ATM	ataxia telangiectasia mutated	1.6	0.0031
CCNH	cyclin H	1.6	0.0021
TFDP1	transcription factor Dp-1	1.4	0.0024
PCNA	proliferating cell nuclear antigen	1.0	0.0251
CDC16	cell division cycle 16	-1.6	0.0007
SERTAD 1	SERTA domain containing 1	-1.8	0.0004
CDKN1B	cyclin-dependent kinase inhibitor 1B	-2.5	<0.0001
DNM2	dynamin 2	-2.5	<0.0001
CDK2	cyclin-dependent kinase 2	-4.1	<0.0001

Table S4. Differential expression of genes involved in immune responses in PIG3V and HEM-l cells

Gene	Gene Description	Log2FC (PIG3V/HEM-l)	p-value
IL7R	interleukin 7 receptor	15.2	<0.0001
TNFSF10	tumor necrosis factor superfamily member 10	13.0	<0.0001
PTGER2	prostaglandin E receptor 2	12.5	<0.0001
HDAC9	histone deacetylase 9	9.4	<0.0001
NFATC1	nuclear factor of activated T-cells 1	9.0	<0.0001
CSF1	colony stimulating factor 1	8.6	<0.0001
CD70	CD70 molecule	8.6	0.0001
FOXP2	forkhead box P2	8.3	0.0002
ITGA1	integrin subunit alpha 1	8.3	<0.0001
HDAC9	histone deacetylase 9	7.7	0.0010
CSF1	colony stimulating factor 1	5.5	<0.0001
TGFB1	transforming growth factor beta 1	4.6	<0.0001
IL6	interleukin 6	3.7	0.0003
FOXP1	forkhead box P1	3.6	0.0068
IL15	interleukin 15	3.3	0.0021
HPRT1	hypoxanthine phosphoribosyltransferase 1	2.6	<0.0001
DGKA	diacylglycerol kinase alpha	2.6	0.0834
ITCH	itchy E3 ubiquitin protein ligase	2.3	<0.0001
MEF2A	myocyte enhancer factor 2A	1.9	0.0670
GAPDH	glyceraldehyde-3-phosphate dehydrogenase	1.8	0.0021
ICAM1	intercellular adhesion molecule 1	1.6	0.0006
CBLB	Cbl proto-oncogene B	1.6	0.0010

Gene	Gene Description	Log2FC (PIG3V/HEM-l)	p-value
FOS	Fos proto-oncogene, AP-1 trancription factor subunit	-1.2	0.0162
STAT6	signal transducer and activator of transcription 6	-1.2	0.0095
NFKB1	nuclear factor kappa B subunit 1	-1.3	0.0161
CDK4	cyclin-dependent kinase 4	-1.3	0.0084
ING4	inhibitor of growth family member 4	-2.2	0.0111
CD40	CD40 molecule	-2.2	0.1880
NOTCH1	notch 1	-2.4	0.0000
CDK2	cyclin-dependent kinase 2	-2.4	0.0002
LGALS3	lectin, galactoside binding soluble 3	-2.8	<0.0001
TNFRSF14	tumor necrosis factor receptor superfamily member 14	-4.8	<0.0001
EOMES	eomesodermin	-5.0	<0.0001
IRF4	interferon regulatory factor 4	-7.6	<0.0001
RNF128	ring finger protein 128, E3 ubiquitin protein ligase	-8.7	<0.0001

Table S5. Changes in major mitochondrial energy metabolism pathway genes in PIG3V cells compared to HEM-l cells

Mitochondrial Complex	Gene	Gene Description	Log2FC (PIG3V/HEM-l)	p-value
Complex1 (NADH-Coenzyme Q reductase)	NDUFC1	NADH:ubiquinone oxidoreductase subunit C1	-4.1	0.0006
	NDUFS7	NADH:ubiquinone oxidoreductase core subunit S7	-2.0	<0.0001
	NDUFB2	NADH:ubiquinone oxidoreductase subunit B2	-1.6	0.0002
	NDUFB7	NADH:ubiquinone oxidoreductase subunit B7	-1.5	0.0004
	NDUFB4	NADH:ubiquinone oxidoreductase subunit B4	-1.5	0.0013
	NDUFB8	NADH:ubiquinone oxidoreductase subunit B8	-1.4	0.0396
	NDUFA11	NADH:ubiquinone oxidoreductase subunit A11	-1.3	0.0046
	NDUFS3	NADH:ubiquinone oxidoreductase core subunit S3	-1.2	0.0028
	NDUFA4	NDUFA4, mitochondrial complex associated	-1.2	0.0215
	NDUFV1	NADH:ubiquinone oxidoreductase core subunit V1	-1.2	0.0099
	NDUFA5	NADH:ubiquinone oxidoreductase subunit A5	1.2	0.0322
Complex II (Succinate-Coenzyme Q reductase)	SDHAF2	succinate dehydrogenase complex assembly factor 1	-1.1	0.0085
	SDHC	succinate dehydrogenase complex subunit C	-0.9	0.0330
Complex IV (Cytochrome c oxidase)	COX6A1	cytochrome c oxidase subunit 6A1	-1.8	0.0006
	COX8A	cytochrome c oxidase subunit 8A	-1.4	0.0035

Table S6 Shotgun lipidomics analysis in HEM-l and PIG3V cells.

Name	HEM-l	PIG3V
Phosphatidylethanolamine(PE)	50.6	55.6
Ceramide (CER)	1.3	1.0
Phosphatidylinositol (PI)	10.0	8.8
Cardiolipin (CL)	0.3	3.7
Phosphatidylserine (PS)	18.8	9.0
Phosphatidylglycerol (PG)	1.7	5.3
Phosphatidic acid (PA)	1.3	0.3
Sphingomyelin (SM)	12.5	5.6
Phosphatidylcholine (PC)	27.0	53.4
Lyso Phosphatidylcholine(LPC)	0.6	1.1
Acyl Carnitine (CAR)	19.5	21.8
Diacylglycerol (DAG)	6.4	2.6
Triacylglycerol (TAG)	11.3	21.7
Fatty Acyl Chains in TAG (FA)	40.4	65.0

Table S7. List of qPCR primer sequences

Gene	Sequence
KIT-F	CGTGGAAAAGAGAAAACAGTCA
KIT-R	CACCGTGATGCCAGCTATTA
MITF-F	AAGGTCTGCCCCCACCAGGC
MITF-R	TTGGCCAGTGCTCTTGCTTCAGAC
TYR -F	CCTAACTTACTCAGCCCAGCA
TYR -R	TGTTGTACTCCTCCAATCGGC
TYRP-1-F	CTTTTCTCACATGGCACAGG
TYRP-1-R	AAGGCTCTTGCAACATTTCC
DCT - F	CCTCAGACCAACTTGGCTACA
DCT - R	GGCCAACCTGGAGTTTCTTC
PMEL-F	TCTTGCTGGTGTTGATGGCT
PMEL-R	GGGGTACGGAGAAGTCTTGC
MLANA-F	CTGCTCATCGGCTGTTGGTA
MLANA-R	GAGCATTGGGAACCACAGGT
TRPM-1-F	ACGACGGAATGGCAATGCCAA
TRPM-1-R	AGGAATTGCTTCAGCGACATGGTG
NRF2-F	AGACGGTATGCAACAGGACA
NRF2-R	GGCTTCTGGACTTGGAACCAT
GPX1 E1- F	ACACCCAGATGAACGAGCTG
GPX1 E2 - R	GCCGGACGTACTTGAGGGAA
TGFBR2 - R	CCAGCACTCAGTCAACGTCT
PPARGC1A -F	ACTTTTGTGGACGCAAGCAA
PPARGC1A -R	GGTGGAAGCAGGGTCAAAGT
IL-7R-F	ATAATAGCTCAGGGGAGATGGA
IL-7R-R	ACTGGGCCATACGATAGGCT
RRM2-F	ACAAGGAGAACACGCCGC
RRM2-R	GGGGGCAGCTGCTTTAGTTT
CCL5-F	AGCAGTCGTCCACAGGTCAA
CCL5-R	CTTCTCTGGGTTGGCACACA
C3-F	TGTGAGCCAGGAGTGGACTA
C3-R	ATCCGAGCCTGACTTGATGG
OAS1-F	GTCGAAGGCCTTGTGAACAG
OAS1-R	CAGTTTGTCAGTCTCCGCCT
IGFBP6-F	CCTGCTGTTGCAGAGGAGAAT
IGFBP6-R	GTCTTGGACACCCGCAGAAT
FOSL1-F	GTCGAAGGCCTTGTGAACAG
FOSL1-R	CAGTTTGTCAGTCTCCGCCT
TAOK1-F	CCTCCTCCTCCTCACTCCTC
TAOK1-R	GGCATAAACTACCTTTCGCCG
HPRT1-F	TGGGACTCTGTAGGGACCAG
HPRT1 - R	GTGATTCAGCCCCAGTCCAT

REFERENCES

Anders S, Huber W. Differential expression analysis for sequence count data. Genome Biol 2010;11:R106.

Cheng H, Guan S, Han X. Abundance of triacylglycerols in ganglia and their depletion in diabetic mice: implications for the role of altered triacylglycerols in diabetic neuropathy. Journal of neurochemistry 2006;97:1288-300.

Das S, Singh S, Dowding JM, Oommen S, Kumar A, Sayle TXT, et al. The induction of angiogenesis by cerium oxide nanoparticles through the modulation of oxygen in intracellular environments. Biomaterials 2012;33:7746-55.

Han X, Gross RW. Shotgun lipidomics: multidimensional MS analysis of cellular lipidomes. Expert review of proteomics 2005;2:253-64.

Mazar J, DeYoung K, Khaitan D, Meister E, Almodovar A, Goydos J, et al. The regulation of miRNA-211 expression and its role in melanoma cell invasiveness. PloS one 2010;5:e13779.

Mazar J, Qi F, Lee B, Marchica J, Govindarajan S, Shelley J, et al. MicroRNA 211 Functions as a Metabolic Switch in Human Melanoma Cells. Molecular and Cellular Biology 2016;36:1090-108.

Mortazavi A, Williams BA, McCue K, Schaeffer L, Wold B. Mapping and quantifying mammalian transcriptomes by RNA-Seq. Nat Methods 2008;5:621-8.

Trapnell C, Pachter L, Salzberg SL. TopHat: discovering splice junctions with RNA-Seq. Bioinformatics 2009;25:1105-11.

Wang M, Wang C, Han X. Selection of internal standards for accurate quantification of complex lipid species in biological extracts by electrospray ionization mass spectrometry—What, how and why? Mass Spectrometry Reviews 2016:n/a-n/a.

Yang K, Cheng H, Gross RW, Han X. Automated lipid identification and quantification by multidimensional mass spectrometry-based shotgun lipidomics. Analytical chemistry 2009;81:4356-68.

Yang K, Han X. Accurate Quantification of Lipid Species by Electrospray Ionization Mass Spectrometry — Meets a Key Challenge in Lipidomics. Metabolites 2011;1:21.